Electron mobility calculation for graphene on substrates

Hirai, Hideki
Tsuchiya, Hideaki
Kamakura, Yoshinari
Mori, Nobuya
Ogawa, Matsuto

(Citation)
Journal of Applied Physics,116(8):083703-083703

(Issue Date)
2014-08-28

(Resource Type)
journal article

(Version)
Version of Record

AIP Journal of Applied Physics

Electron mobility calculation for graphene on substrates

Hideki Hirai, Hideaki Tsuchiya, Yoshinari Kamakura, Nobuya Mori, and Matsuto Ogawa

Citation: Journal of Applied Physics **116**, 083703 (2014); doi: 10.1063/1.4893650
View online: http://dx.doi.org/10.1063/1.4893650
View Table of Contents: http://scitation.aip.org/content/aip/journal/jap/116/8?ver=pdfcov
Published by the AIP Publishing

Electron mobility calculation for graphene on substrates

Hideki Hirai,[1] Hideaki Tsuchiya,[1,2,a)] Yoshinari Kamakura,[2,3] Nobuya Mori,[2,3] and Matsuto Ogawa[1]

[1]*Department of Electrical and Electronic Engineering, Graduate School of Engineering, Kobe University, 1-1, Rokko-dai, Nada-ku, Kobe 657-8501, Japan*
[2]*Japan Science and Technology Agency, CREST, Chiyoda, Tokyo 102-0075, Japan*
[3]*Division of Electrical, Electronic and Information Engineering, Graduate School of Engineering, Osaka University, Suita, Osaka 565-0871, Japan*

(Received 20 May 2014; accepted 7 August 2014; published online 22 August 2014)

By a semiclassical Monte Carlo method, the electron mobility in graphene is calculated for three different substrates: SiO_2, HfO_2, and hexagonal boron nitride (h-BN). The calculations account for polar and non-polar surface optical phonon (OP) scatterings induced by the substrates and charged impurity (CI) scattering, in addition to intrinsic phonon scattering in pristine graphene. It is found that HfO_2 is unsuitable as a substrate, because the surface OP scattering of the substrate significantly degrades the electron mobility. The mobility on the SiO_2 and h-BN substrates decreases due to CI scattering. However, the mobility on the h-BN substrate exhibits a high electron mobility of 170 000 $cm^2/(V\cdot s)$ for electron densities less than $10^{12}\,cm^{-2}$. Therefore, h-BN should be an appealing substrate for graphene devices, as confirmed experimentally. © *2014 AIP Publishing LLC*.
[http://dx.doi.org/10.1063/1.4893650]

I. INTRODUCTION

Graphene, a two-dimensional (2D) sheet of carbon atoms in a honeycomb lattice, is promising for device applications as it has a high intrinsic mobility, even at room temperature. Experimentally, graphene layers decoupled from bulk graphite have been demonstrated to exhibit carrier mobilities exceeding 10^7 $cm^2/(V\cdot s)$ at temperatures up to $T = 50$ K.[1] A full-band Monte Carlo simulation using the electron-phonon interaction in graphene described by density-functional perturbation theory[2] has predicted an intrinsic mobility of approximately 5×10^6 $cm^2/(V\cdot s)$ at $T = 50$ K, in reasonable agreement with these experimental results. On the other hand, at $T = 300$ K the simulation predicts a mobility of 9.5×10^5 $cm^2/(V\cdot s)$, which is much higher than expected.

Although practical applications of a graphene field-effect transistor (FET) require a reliable substrate, the mobility in graphene on SiO_2 substrates is limited to 25 000 $cm^2/(V\cdot s)$.[3–5] The reason for this mobility reduction on SiO_2 substrates is the additional scattering mechanisms induced by the substrate, including charged impurities,[6–8] polar and non-polar surface optical phonons (OPs) in the SiO_2,[7,9,10] and substrate surface roughness.[11,12] Recently, a drastic improvement of the mobility to 140 000 $cm^2/(V\cdot s)$ near the charge neutrality point was achieved using a hexagonal boron nitride (h-BN) substrate.[13] That substrate has an atomically smooth surface with minimal dangling bonds and charge traps. It also has a lattice constant similar to that of graphite, and a large optical phonon energy and bandgap. Recently, it has been reported that h-BN exhibits potential fluctuations due to charged impurities that are one or two orders of magnitude lower than in SiO_2.[14] Based on these results, h-BN substrate is a suitable substrate for graphene devices.

In the present paper, the electron mobility in graphene on various substrates is calculated by considering surface OP and charged impurity (CI) scattering induced by the substrates, as well as the intrinsic acoustic phonon (AP) and OP scattering in pristine graphene. The substrates considered are SiO_2, HfO_2, and h-BN, which are technologically important substrates and gate insulators. Surface AP scattering, which plays an important role in piezoelectric substrates, is not considered in this study. The electron mobility is calculated using a semiclassical Monte Carlo approach,[15,16] in which both the linear dispersion relation of the graphene and the Pauli exclusion principle are taken into account. The electron density dependence of the mobility is investigated, and comparisons with experimental results are performed to identify the main scattering mechanism leading to the mobility reduction in graphene on the substrates.

II. SIMULATION METHOD

Figure 1 is a schematic of the graphene-on-substrate system considered in this study. A uniform electric field E_x is applied along the x-direction. Electron transport in a

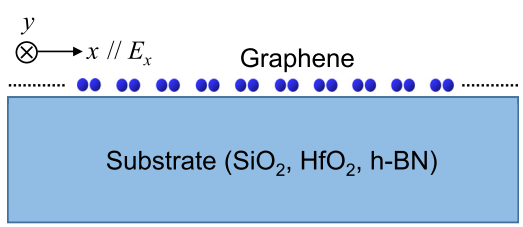

FIG. 1. Schematic of the graphene-on-substrate system considered in this study. A uniform electric field E_x is applied along the x-direction. Three kinds of substrates (SiO_2, HfO_2, and h-BN) are investigated.

a)Author to whom correspondence should be addressed. Electronic mail: tsuchiya@eedept.kobe-u.ac.jp. Tel./Fax: +81-78-803-6082.

monolayer graphene on the three substrates (SiO_2, HfO_2, and h-BN) is analyzed using a Monte Carlo simulator for uniform transport, as described below.

A. Band structure

For graphene, the gapless energy dispersion relation at the K_1 and K_2 points is approximated by the equation

$$E_{\mathbf{k}} = \hbar v_f |\mathbf{k}|, \tag{1}$$

where $v_f = 10^8\,\mathrm{cm/s}$ is the Fermi velocity and $|\mathbf{k}|$ is the magnitude of the 2D wavevector relative to the K_1 and K_2 points in **k**-space.

B. Scattering mechanisms

The AP, OP, and CI scattering mechanisms are assumed to be isotropic.[17] The elastic AP and inelastic OP (with $\hbar\omega_{\mathrm{op}} = 164\,\mathrm{meV}$) cause an intravalley transition $K_{1(2)} \rightarrow K_{1(2)}$, whereas the inelastic AP (with $\hbar\omega_{\mathrm{ac}} = 124\,\mathrm{meV}$) results in an intervalley transition $K_{1(2)} \rightarrow K_{2(1)}$ in intrinsic graphene.[2] These are here called the intrinsic AP and OP in graphene. Their scattering rates are given by[17–19]

$$S_{\mathrm{ac}}^{\mathrm{elas}} = \frac{E_D^2 k_B T}{4\hbar^3 v_f^2 v_s^2 \rho_s} E, \tag{2}$$

for elastic AP scattering, where a density of $\rho_s = 7.6 \times 10^{-8}\,\mathrm{g/cm^2}$ and a sound velocity of $v_s = 2 \times 10^6\,\mathrm{cm/s}$ are assumed here, and by

$$S_{\mathrm{op\,(ac)}}^{\mathrm{inelas}} = \frac{D_f^2}{\hbar^2 \omega_s\, \omega_{\mathrm{op\,(ac)}} v_f^2} \left[\left(E - \hbar\omega_{\mathrm{op\,(ac)}}\right) \left(N_{\hbar\omega_{\mathrm{op\,(ac)}}} + 1\right) \times \Theta\left(E - \hbar\omega_{\mathrm{op\,(ac)}}\right) + \left(E + \hbar\omega_{\mathrm{op\,(ac)}}\right) N_{\hbar\omega_{\mathrm{op\,(ac)}}} \right], \tag{3}$$

for inelastic OP and AP scattering. $\Theta(x)$ is the Heaviside function. In other words, $\Theta = 1$ for $x \geq 1$ and zero otherwise. The function $\Theta(x)$ ensures that the energy is sufficient to emit a phonon. Parameters for the phonon scattering rates are summarized in Table I. For the deformation potential E_D in Eq. (2), a value of 4.5 eV is used, whereas for the deformation field D_f in Eq. (3), values of $1.0 \times 10^9\,\mathrm{eV/cm}$ and $3.5 \times 10^8\,\mathrm{eV/cm}$ are used for the intrinsic OP and AP in graphene, respectively.[2] These values are determined by approximating the *ab initio* electron-phonon scattering rates using the simple analytical formulae of Eqs. (2) and (3), where E_D and D_f are treated as effective quantities to determine the contribution of all the relevant phonon scatterings.

The OP and CI scatterings induced by the substrates are introduced as follows. First, in semiclassical Monte Carlo studies, it is convenient to use the deformation potential approximation in estimating the scattering rates of various mechanisms.[17–19] The scattering rates of the polar and non-polar surface OPs in the substrates are comparable to or larger than those of the intrinsic AP and OP, and thus they may reduce the effects from the intrinsic phonon scattering.[19] These scattering mechanisms are approximately modeled using Eq. (3) with the polar and non-polar surface OPs merged. In fact, the approach has successfully reproduced experimental electron velocity versus electric field curves by adjusting the deformation field D_f in Eq. (3), as reported in Ref. 19. Therefore, the resultant D_f for the surface OP scatterings represents an effective interaction strength between the electrons in graphene and the surface OPs including the non-polar one, so as to reproduce the experimental results. This approach is simple and efficient, and hence, it has been widely used to simulate electron transport of graphene as in Refs. 17–19 and 21, where velocity saturation in zero-bandgap graphene FETs has been discussed based on the surface OP energy of substrates.[22,23] On the other hand, a more rigorous approach where the polar surface OP scattering was modeled using a long-range polarization field created at the graphene and substrate interface has been also proposed.[10,24,25] As far as we know, essentially, the same electron density dependency of the electron mobility has been obtained by using the two approaches.[17,18,21,24] Thus, we deem the present approach to be applicable to the analysis of the electron mobility for graphene on the polar substrates.

The parameters of the surface OP scattering used in the simulation are listed in the lower part of Table I. The surface OP energies of SiO_2, HfO_2, and h-BN are 55, 12.4, and 200 meV, respectively,[20,21] and the deformation fields for SiO_2 and HfO_2 are given by $5.14 \times 10^7\,\mathrm{eV/cm}$ and $1.29 \times 10^9\,\mathrm{eV/cm}$, respectively, which give the best match with the experimental electron velocity versus electric field curves,[19] as mentioned above. However, the deformation field for h-BN is unknown. So, it is varied from $1 \times 10^6\,\mathrm{eV/cm}$ to $1.29 \times 10^9\,\mathrm{eV/cm}$, spanning the range of the deformation

TABLE I. Parameters of the phonon scattering rates and values of the charged impurity densities.

Electron-phonon interaction parameters of graphene[2]			
Optical phonon energy $\hbar\omega_{\mathrm{op}}$ (meV)			164
Intervalley acoustic phonon energy $\hbar\omega_{\mathrm{ac}}$ (meV)			124
Deformation potential of acoustic phonon E_D (eV)			4.5
Deformation field of optical phonon D_f (eV/cm)			1.0×10^9
Deformation field of intervalley acoustic phonon D_f (eV/cm)			3.5×10^8
Parameters of the surface optical phonon and of the charged impurity in substrates			
	SiO_2	HfO_2	h-BN
Optical phonon energy $\hbar\omega_{\mathrm{op}}$ (meV)	55 (Ref. 20)	12.4 (Ref. 20)	200 (Ref. 21)
D_f of optical phonon (eV/cm)	5.14×10^7 (Ref. 19)	1.29×10^9 (Ref. 19)	1.0×10^6–1.29×10^9
Charged impurity density n_{imp} ($\mathrm{cm^{-2}}$)	2.5×10^{11} (Ref. 14)	…	2.5×10^{10} (Ref. 14)

fields for SiO_2 and HfO_2. The results indicate that the electron mobility for h-BN is independent of the value of the deformation fields. Therefore, results will be shown for the h-BN substrate obtained using the largest deformation field, 1.29×10^9 eV/cm. Scattering due to charged impurities in the substrates is taken into account by using the equation[17–19]

$$S_{\text{imp}} = \frac{h v_f^2 n_{\text{imp}}}{20E}, \tag{4}$$

assuming that the impurities are homogeneously distributed throughout the substrates with a fixed sheet density n_{imp}. The 2D charge density in SiO_2 substrate has been reported[14] to range from 0.24 to $2.7 \times 10^{11}\,\text{cm}^{-2}$, whereas h-BN exhibits potential fluctuations due to charged impurities that are one to two orders of magnitude lower than in SiO_2. Accordingly, n_{imp} is taken to be $2.5 \times 10^{11}\,\text{cm}^{-2}$ and $2.5 \times 10^{10}\,\text{cm}^{-2}$ for SiO_2 and h-BN, respectively. Graphene on HfO_2 with charged impurities is not simulated, for reasons given in Sec. III. In the meantime, some other experimental electron mobilities in graphene on substrates[26–28] were reported to be significantly smaller than the values of the present study, and hence scattering mechanisms such as the surface piezoelectric AP scattering may need to be considered to reproduce such lower electron mobilities of graphene-on-substrate samples.

C. Carrier degeneracy

The Pauli exclusion principle for the scattering final state is treated using a rejection technique[29] described below. Following a scattering event, the new state is accepted or rejected with a probability that depends on the carrier distribution function in energy. The low-field electron mobility is examined, so that the carrier distribution can be approximated by the equilibrium Fermi-Dirac function with lattice temperature T and Fermi energy E_F. The relation between the electron density and Fermi energy is needed to determine the electron density dependence of the mobility. Using the Fermi-Dirac function and the graphene density of states for electrons given by

$$g(E) = \frac{2E}{\pi \hbar^2 v_f^2}, \tag{5}$$

the Fermi energies are calculated for various electron densities relevant to FET operation at $T = 300$ K, as listed in Table II. It is seen that graphene has a Fermi energy exceeding a few hundred meV at reasonable densities, and therefore, consideration of the carrier degeneracy is necessary.

The general semiclassical Monte Carlo approach described in Refs. 15 and 16 is employed. Various parameters, such as the average velocity and average energy, are computed by taking an ensemble average over the particles involved in the transport. Here, an ensemble of 10^5 particles is considered. The electric field E_x is 0.01 kV/cm, sufficiently small to maintain an equilibrium state of the electrons.

TABLE II. Fermi energies for various electron densities at $T = 300$ K.

Density (cm^{-2})	Fermi energy (meV)
5×10^{11}	69
1×10^{12}	107
2×10^{12}	159
5×10^{12}	257
8×10^{12}	327
1×10^{13}	366

III. ELECTRON MOBILITY CONSIDERING SURFACE OPTICAL PHONON SCATTERING OF SUBSTRATES

Figure 2 shows the electron mobility computed as a function of the electron density n at $T = 300$ K, where CI scattering was not included. The "intrinsic" case only considers intrinsic AP and OP scatterings. The inset is a magnified view of the results for graphene on HfO_2. The largest deformation field ($D_f = 1.29 \times 10^9$ eV/cm) is used for the surface OP scattering of h-BN. Graphene on SiO_2 and h-BN has almost the same electron mobility as the intrinsic case, whereas the graphene on HfO_2 exhibits a mobility that is about three orders of magnitude smaller than the others. The drastic reduction in the mobility on the HfO_2 substrate is due to its small surface OP energy of 12.4 meV and its large deformation field, as listed in Table I. When the surface OP energy is smaller than the thermal energy $k_B T \approx 26$ meV at $T = 300$ K, the electrons distributed around the Fermi energy can be scattered by the surface OP because the Pauli exclusion principle has limited influence.

The negligible reduction in the electron mobility for the SiO_2 and h-BN substrates is explained as follows. The h-BN substrate has a large surface OP energy of 200 meV. Accordingly, the Pauli exclusion principle suppresses most of the surface OP scattering, thereby leading to minimal reduction in the electron mobility. On the other hand, the surface OP energy of the SiO_2 substrate is 55 meV, which is not large enough to suppress the surface OP scattering by the Pauli exclusion principle at $T = 300$ K. Then, the rates for each phonon scattering mechanism on a SiO_2 substrate are plotted in Fig. 3, where the scattering rates for surface OP scattering are plotted by the solid blue curve (for the surface

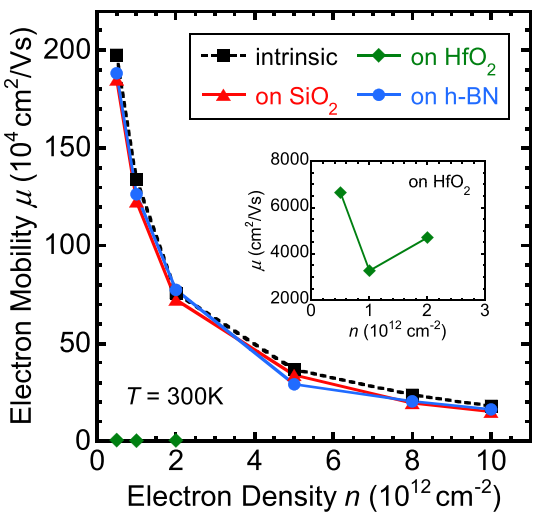

FIG. 2. Electron mobility computed as a function of the electron density n at $T = 300$ K, not including charged impurity scattering. The "intrinsic" case only considers intrinsic AP and OP scatterings. The inset plots a magnified view of the results for graphene on HfO_2.

OP emission process) and by the dashed blue curve (for the surface OP absorption process). These rates are significantly smaller than the intrinsic AP and OP emission rates in the low- and high-energy regions, respectively. Consequently, electrons in graphene on a SiO_2 substrate are hardly affected by a surface OP, explaining the negligible reduction in the electron mobility. As already mentioned, a surface OP in a SiO_2 or h-BN substrate has little impact on the electron mobility in graphene. However, graphene on HfO_2 suffers from significant surface OP scattering, so that HfO_2 is unsuitable as a substrate of graphene. Hereafter, analysis of only the SiO_2 and h-BN substrates is pursued.

As seen in Fig. 2, the Monte Carlo simulation predicts a large intrinsic mobility of approximately 2×10^6 $cm^2/(V \cdot s)$ for $n < 10^{12}\,cm^{-2}$, in good agreement with Ref. 2. However, the mobility drastically decreases by about an order of magnitude as n increases to $10^{13}\,cm^{-2}$. Similar results have been reported in the literature[17,18,21,24] and have been explained using the Pauli exclusion principle. To demonstrate the effect using a practical carrier distribution, the particle distributions are plotted in 2D **k**-space in Fig. 4 for densities of (a) $5 \times 10^{11}\,cm^{-2}$ and (b) $10^{13}\,cm^{-2}$, where only the intrinsic AP and OP in graphene are considered. The point $k_x = k_y = 0$ represents the Dirac point. The electric field is applied in the x-direction. As n increases, the Fermi energy is pushed above the Dirac point due to the Pauli exclusion principle, as shown in Fig. 4(b). Since the mobility is mainly determined by electronic states close to the Fermi energy and the raised Fermi energy increases the corresponding scattering rates, the mobility decreases with an increase in the electron density. This mobility decrease with increasing electron density may lead to a performance degradation of graphene FETs in the on state.

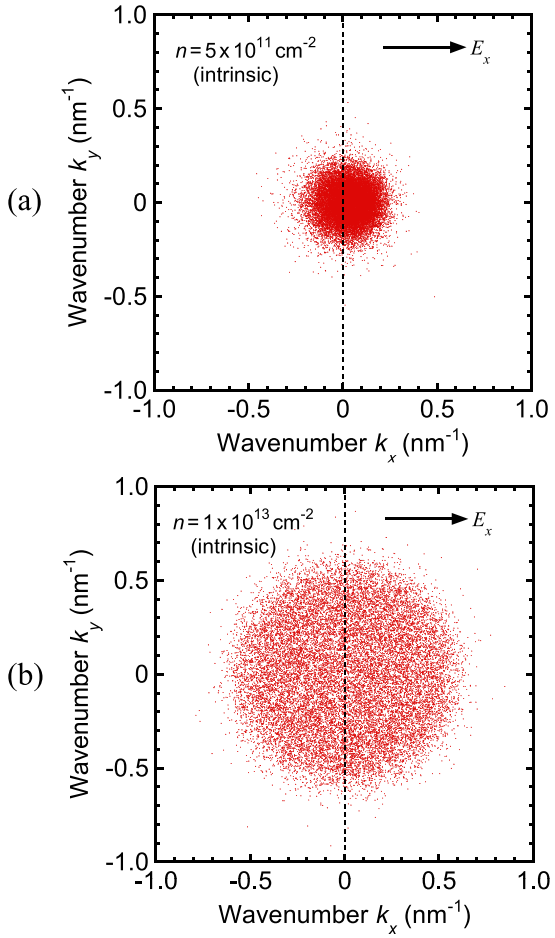

FIG. 4. Particle distributions in 2D **k**-space obtained by Monte Carlo simulations for (a) $n = 5 \times 10^{11}\,cm^{-2}$ and (b) $n = 10^{13}\,cm^{-2}$, accounting only for the intrinsic AP and OP in graphene. The point $k_x = k_y = 0$ is the Dirac point. The electric field is applied along the x-direction.

IV. ELECTRON MOBILITY CONSIDERING CHARGED IMPURITY SCATTERING

From the results of Sec. III, surface OP scattering for SiO_2 and h-BN has little impact on the electron mobility in graphene. Hence, it is ignored in the following calculations. Instead, CI scattering from the substrates is included.

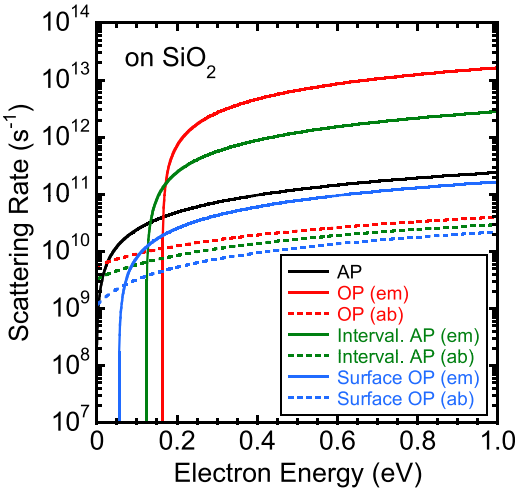

FIG. 3. Scattering rates computed as a function of electron energy for all phonon scattering mechanisms on a SiO_2 substrate. The rates for surface OP scattering are plotted as the solid blue curve (for the surface OP emission process) and as the dashed blue curve (for the surface OP absorption process).

The strength of the CI scattering depends on the 2D charge density n_{imp} in the substrates. Based on the experimental analysis of Ref. 14, in which h-BN exhibits potential fluctuations due to charged impurities that are one or two orders of magnitude lower than for SiO_2, the value of n_{imp} is taken to be $2.5 \times 10^{11}\,cm^{-2}$ and $2.5 \times 10^{10}\,cm^{-2}$ for SiO_2 and h-BN substrates, respectively. Figure 5 shows the computed electron mobility when CI scattering is considered, along with the results for the "intrinsic" case for comparison. The mobility for both substrates is considerably decreased by CI scattering. In particular, the mobility on a SiO_2 substrate decreases to $20\,000\,cm^2/(V \cdot s)$, in good agreement with experimental measurements in Refs. 3–5, and it is nearly independent of the electron density. Charged impurity scattering has an increasing influence on the electrons as their kinetic energy decreases, as shown in Fig. 6, where the CI scattering rates for $n_{imp} = 2.5 \times 10^{11}\,cm^{-2}$ (on SiO_2) and $2.5 \times 10^{10}\,cm^{-2}$ (on h-BN) are plotted, together with those for intrinsic phonon scattering. When the electron density is small, electrons in graphene are heavily scattered by charged impurities, because the Fermi energy is then small (cf. Table II). As a result, the electron mobility drastically decreases

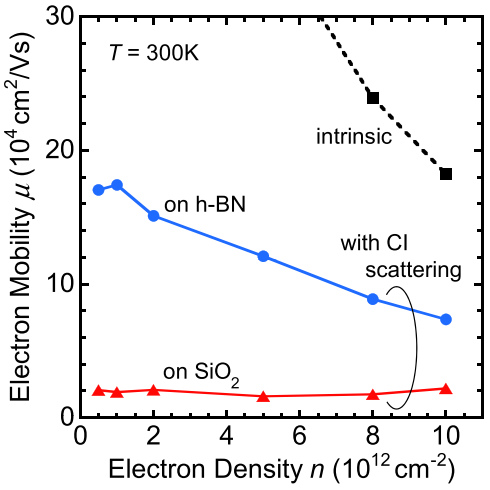

FIG. 5. Electron mobility computed by considering charged impurity scattering and ignoring surface OP scattering of the substrates. Here, n_{imp} is taken to be $2.5 \times 10^{11}\,cm^{-2}$ and $2.5 \times 10^{10}\,cm^{-2}$ for the SiO_2 and h-BN substrates, respectively. The results for the "intrinsic" case are plotted as the dashed line for comparison.

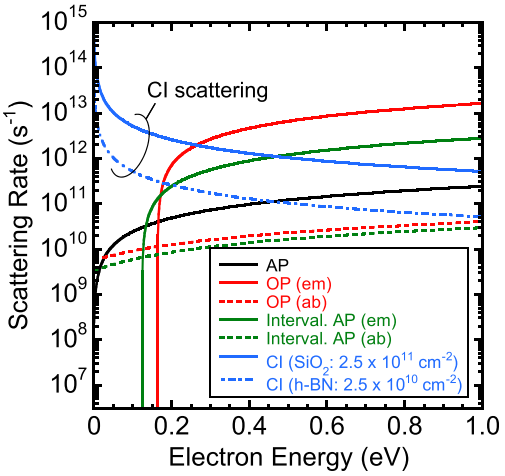

FIG. 6. Charged impurity scattering rates for $n_{imp} = 2.5 \times 10^{11}\,cm^{-2}$ (on SiO_2) and $2.5 \times 10^{10}\,cm^{-2}$ (on h-BN), along with those for intrinsic phonon scattering. The charged impurity scattering has increasing influence on the electrons as their kinetic energy becomes smaller.

with decreasing electron density, and thus, no electron density dependence of the mobility is observed in a SiO_2 substrate with charged impurities.

The mobility on a h-BN substrate is $170\,000\,cm^2/(V{\cdot}s)$ for $n < 10^{12}\,cm^{-2}$, which agrees with Ref. 13. This mobility arises from the smaller value of n_{imp} in the h-BN substrate, as confirmed by the smaller CI scattering rate in Fig. 6. Therefore, the recently observed high electron mobility of $140\,000\,cm^2/(V{\cdot}s)$ for a h-BN substrate[14] can be confirmed to be due to its small charged impurity density. Therefore, a h-BN substrate is an appealing choice for graphene devices.

V. CONCLUSION

Using a semiclassical Monte Carlo method, the electron mobility in graphene on three different substrates, SiO_2, HfO_2, and h-BN, has been calculated by considering the extrinsic scattering due to the surface OP and charged impurities in the substrates, as well as the intrinsic phonon scattering in the graphene. By investigating the influence of the surface OP scattering, HfO_2 was shown to be unsuitable as a substrate for graphene. On the other hand, the surface OP in the SiO_2 and h-BN substrates was found to have little impact on the electron mobility in graphene. Therefore, these two substrates were further examined by considering scattering due to charged impurities in the substrates. The mobility for both substrates decreases by CI scattering, but the mobility for the h-BN substrate maintains a relatively high value of $170\,000\,cm^2/(V{\cdot}s)$ for electron densities below $10^{12}\,cm^{-2}$. This result was confirmed as being due to the smaller charged impurity density in the h-BN substrate. Good agreement is found between the calculated results and the experimental measurements. For the SiO_2 and h-BN substrates, the main scattering mechanism leading to mobility reduction is charged impurities in the substrates, and in that context, h-BN substrate is the best choice for graphene devices.

ACKNOWLEDGMENTS

This work was supported by a Grant-in-Aid for Scientific Research from the Japanese Society for the Promotion of Science (JSPS) and the Japanese Science and Technology Agency (JST/CREST).

[1]P. Neugebauer, M. Orlita, C. Faugeras, A.-L. Barra, and M. Potemski, Phys. Rev. Lett. **103**, 136403 (2009).
[2]K. M. Borysenko, J. T. Mullen, E. A. Barry, S. Paul, Y. G. Semenov, J. M. Zavada, M. Buongiorno Nardelli, and K. W. Kim, Phys. Rev. B **81**, 121412 (2010).
[3]Y.-W. Tan, Y. Zhang, K. Bolotin, Y. Zhao, S. Adam, E. H. Hwang, S. Das Sarma, H. L. Stormer, and P. Kim, Phys. Rev. Lett. **99**, 246803 (2007).
[4]S. Cho and M. S. Fuhrer, Phys. Rev. B **77**, 081402 (2008).
[5]J. Yan and M. S. Fuhrer, Phys. Rev. Lett. **107**, 206601 (2011).
[6]E. Rossi, S. Adam, and S. Das Sarma, Phys. Rev. B **79**, 245423 (2009).
[7]J.-H. Chen, C. Jang, S. Xiao, M. Ishigami, and M. S. Fuhrer, Nat. Nanotechnol. **3**, 206 (2008).
[8]J. Martin, N. Akerman, G. Ulbricht, T. Lohmann, J. H. Smet, K. von Klitzing, and A. Yacoby, Nat. Phys. **4**, 144 (2008).
[9]E. H. Hwang and S. Das Sarma, Phys. Rev. B **77**, 115449 (2008).
[10]S. Fratini and F. Guinea, Phys. Rev. B **77**, 195415 (2008).
[11]M. Ishigami, J.-H. Chen, W. G. Cullen, M. S. Fuhrer, and E. D. Williams, Nano Lett. **7**, 1643 (2007).
[12]S. V. Morozov *et al.*, Phys. Rev. Lett. **100**, 016602 (2008).
[13]C. R. Dean, A. F. Young, I. Meric, C. Lee, L. Wang, S. Sorgenfrei, K. Watanabe, T. Taniguchi, P. Kim, K. L. Shepard, and J. Hone, Nature Nanotechnol. **5**, 722 (2010).
[14]K. M. Burson, W. G. Cullen, S. Adam, C. R. Dean, K. Watanabe, T. Taniguchi, P. Kim, and M. S. Fuhrer, Nano Lett. **13**, 3576 (2013).
[15]C. Jacoboni and L. Reggiani, Rev. Mod. Phys. **55**, 645 (1983).
[16]N. Harada, Y. Awano, S. Sato, and N. Yokoyama, J. Appl. Phys. **109**, 104509 (2011).
[17]J. Chauhan and J. Guo, Appl. Phys. Lett. **95**, 023120 (2009).
[18]R. S. Shishir and D. K. Ferry, J. Phys. Condens. Matter **21**, 344201 (2009).
[19]J. K. David, L. F. Register, and S. K. Banerjee, IEEE Trans. Electron Devices **59**, 976 (2012).
[20]T. O'Regan and M. Fischetti, Jpn. J. Appl. Phys. **46**, 3265 (2007).
[21]D. K. Ferry, in 12th IEEE International Conference on Nanotechnology (IEEE-NANO), Birmingham, 20–23 August (2012).
[22]I. Meric, C. R. Dean, A. F. Young, N. Baklitskaya, N. J. Tremblay, C. Nuckolls, P. Kim, and K. L. Shepard, Nano Lett. **11**, 1093 (2011).
[23]I. Meric, M. Y. Han, A. F. Young, B. Ozyilmaz, P. Kim, and K. L. Shepard, Nat. Nanotechnol. **3**, 654 (2008).

[24]M. Bresciani, P. Palestri, D. Esseni, L. Selmi, B. Szafranek, and D. Neumaier, Solid-State Electron. **89**, 161 (2013).
[25]V. Perebeinos and P. Avouris, Phys. Rev. B **81**, 195442 (2010).
[26]L. Liao, J. Bai, Y. Qu, Y. Huang, and X. Duan, Nanotechnology **21**, 015705 (2010).
[27]I. Meric, C. Dean, A. Young, J. Hone, P. Kim, and K. L. Shepard, IEEE Int. Electron Dev. Meet. **2010**, 556.
[28]A. Y. Serov, Z.-Y. Ong, M. V. Fischetti, and E. Pop, J. Appl. Phys. **116**, 034507 (2014).
[29]M. V. Fischetti and S. E. Laux, Phys. Rev. B **38**, 9721 (1988).